

# On the Lanthanide Ferrocyanides $KLnFe(II)(CN)_6 \cdot xH_2O$ ( $Ln=La-Lu$ ): Characterization and Thermal Evolution

Fabrice Goubard<sup>1</sup> and Alain Tabuteau

Laboratoire de Chimie des Matériaux Inorganiques, Université de Cergy-Pontoise, 5 Mail Gay-Lussac, Neuville sur Oise, 95031 Cergy-Pontoise Cedex, France

Received November 16, 2001; in revised form March 26, 2002; accepted April 12, 2002

The properties of a series of lanthanide hexacyanoferrate(II)  $n$ -hydrates were studied by thermal analysis, IR spectroscopy and X-ray diffraction. Thermal analysis results show that there are three kinds of complexes in this series,  $KLn[Fe(CN)_6] \cdot 4H_2O$  ( $Ln=La-Nd$ ),  $KSm[Fe(CN)_6] \cdot 3H_2O$  and  $KLn[Fe(CN)_6] \cdot 3.5H_2O$  ( $Ln=Eu-Lu$ ). On the basis of IR spectra, only two different types of complexes show obvious differences. Indeed for the tetrahydrates, there is one OH stretching band; on the other hand, for the samarium phase and the 3.5 hydrates a splitting of HOH stretching mode is observed. The splitting of the  $H_2O$  band is correlated to a symmetry modification. The crystal structures of the three complexes  $KLn[Fe(CN)_6] \cdot 3.5H_2O$  ( $Ln=Eu, Er$  and  $Lu$ ) were determined; they belong to orthorhombic symmetry (space group  $Cmcm$ ). Heat-treated powders have been investigated by X-ray analysis which show the formation of thin needles of  $LnFeO_3$  at  $600^\circ C$ . © 2002 Elsevier Science (USA)

**Key Words:** heteronuclear cyano complex; lanthanide; ternary oxide; structure determination.

## 1. INTRODUCTION

Prandtl and Mohr (1) first reported the preparation of several double salts of alkali-lanthanide ferrocyanides, where the alkali metals were sodium and potassium (lanthanide=La, Pr, Nd, Sm, Eu, Gd, Tb, Dy and Er). With the larger rare earth elements ( $Ln=La-Nd$ ), these salts crystallize in the hexagonal  $P6_3/m$  space group (2–5) which is a substitution derivative of the hexagonal  $LaFe(CN)_6 \cdot 5H_2O$  (6) in which half of the uncoordinated water molecules are statistically replaced by potassium ions. The next basis member of the series  $KSmFe(CN)_6 \cdot 3H_2O$  crystallizes in the monoclinic  $P2_1/m$  space group (7), whereas the ferrocyanide hydrate  $KYb-$

$Fe(CN)_6$  contains only 3.5  $H_2O$  [half of one of the three coordinated water molecules is missing and the slightly rearranged structure is now orthorhombic,  $Cmcm$  space group (8)].

In the field of the ceramic elaboration there is a need of a chemical processing method which would both include a lowering of the synthesis temperature and lead to an improvement in the homogeneity and reproducibility of the resulting ceramic products. To that end, pure  $LaFeO_3$  powders, with ultrafine and homogeneous particles, were prepared by thermal decomposition at low temperature (9).

This work is part of our investigation program of double salts of potassium ferrocyanide with rare earth elements. We report here on the synthesis and properties of hexaferrocyanides and on the structural determination of  $KLnFe(CN)_6 \cdot 3.5H_2O$  ( $Ln=Eu, Er, Lu$ ).

Moreover, a systematic investigation of the structural evolution with temperature of the cyanide-bridged heteronuclear complex  $KLnFe(CN)_6 \cdot xH_2O$ , which leads to the formation of  $LnFeO_3$  powders is reported. A comparison with the thermal oxydation of  $NH_4LnFe(CN)_6 \cdot xH_2O$  is discussed and finally, thermal evolution in ammonia and nitrogen atmosphere of these compounds is also shown.

## 2. EXPERIMENTAL SECTION

### 2.1. Materials and Preparation

The iron lanthanide cyanides  $KLnFe(CN)_6 \cdot xH_2O$  ( $Ln=La-Lu$ ) were synthesized by mixing aqueous solutions of  $K_4Fe(CN)_6 \cdot 4H_2O$  and  $Ln(NO_3)_3 \cdot 6H_2O$  or  $TbCl_3 \cdot 6H_2O$ . Each mixture was stirred under reflux for 6 days. The fine and microcrystalline powder was filtered off, washed and dried in air. No single crystal could be found in the bulk samples. The same procedure was used to synthesize  $NH_4LnFe(CN)_6 \cdot xH_2O$  from  $(NH_4)_4Fe(CN)_6 \cdot 4H_2O$ .

<sup>1</sup>To whom correspondence should be addressed. Fax: (33) 1-34-25-70-71. E-mail: fabrice.goubard@chim.u-cergy.fr.

**TABLE 1**  
**Crystal Data, Conventional Rietveld Factors, Positional and Isotropic Thermal Parameters for the Three Structural Refinements**

	<i>Ln</i> =Eu	<i>Ln</i> =Er	<i>Ln</i> =Lu
<i>a</i> (Å)	7.2938(3)	7.2330(3)	7.2256(3)
<i>b</i> (Å)	12.5456(5)	12.4885(4)	12.4639(4)
<i>c</i> (Å)	13.6551(5)	13.4964(4)	13.4143(4)
<i>V</i> (Å <sup>3</sup> )	1249.5	1219.1	1208.1
<i>R</i> <sub>P</sub>	7.43	6.96	7.29
<i>R</i> <sub>WP</sub>	13.58	12.48	13.89
<i>R</i> <sub>B</sub>	5.35	4.82	5.47
<i>R</i> <sub>F</sub>	5.94	5.02	5.84
<i>Ln</i> (0, <i>y</i> , 0.25) (4 <i>c</i> ) <i>y</i>	0.3409(2)	0.3417(2)	0.3405(2)
Occupancy: 1.00 <i>B</i> (Å <sup>2</sup> )	0.28(3)	0.42(3)	0.58(3)
Fe (0, 0, 0) (4 <i>a</i> ) <i>B</i> (Å <sup>2</sup> )	1.49(7)	1.53(7)	1.36(5)
Occupancy: 1.00			
C(1) ( <i>x</i> , <i>y</i> , <i>z</i> ) (16 <i>h</i> ) <i>x</i>	0.312(2)	0.314(2)	0.313(2)
Occupancy: 1.00 <i>y</i>	0.437(2)	0.434(2)	1.435(2)
<i>z</i>	0.078(1)	0.081(1)	0.080(1)
<i>B</i> (Å <sup>2</sup> )	0.601(3)	0.670(3)	0.972(3)
C(2) (0, <i>y</i> , <i>z</i> ) (8 <i>f</i> ) <i>y</i>	0.120(2)	0.119(2)	0.121(2)
Occupancy: 1.00 <i>z</i>	0.090(2)	0.087(2)	0.086(2)
<i>B</i> (Å <sup>2</sup> )	0.6(1)	0.82(9)	0.85(9)
N(1) ( <i>x</i> , <i>y</i> , <i>z</i> ) (16 <i>h</i> ) <i>x</i>	0.203(2)	0.202(2)	0.202(2)
Occupancy: 1.00 <i>y</i>	0.399(2)	0.392(1)	0.391(1)
<i>z</i>	0.126(1)	0.127(1)	0.125(1)
<i>B</i> (Å <sup>2</sup> )	2.0(4)	2.2(3)	2.2(3)
N(2) (0, <i>y</i> , <i>z</i> ) (8 <i>f</i> ) <i>y</i>	0.192(2)	0.189(2)	0.188(2)
Occupancy: 1.00 <i>z</i>	0.144(2)	0.145(1)	0.145(2)
<i>B</i> (Å <sup>2</sup> )	0.9(4)	1.4(3)	1.0(3)
O(1) (0, <i>y</i> , <i>z</i> ) (8 <i>f</i> ) <i>y</i>	0.656(5)	0.662(6)	0.661(6)
Occupancy: 0.50 <i>z</i>	0.083(8)	0.087(7)	0.088(7)
<i>B</i> (Å <sup>2</sup> )	2.6(9)	3.2(9)	2.6(9)
K (0, <i>y</i> , <i>z</i> ) (8 <i>f</i> ) <i>y</i>	0.663(2)	0.664(2)	0.667(2)
Occupancy: 0.50 <i>z</i>	0.081(3)	0.081(2)	0.080(2)
<i>B</i> (Å <sup>2</sup> )	1.2(3)	1.4(3)	1.8(3)
O(2) ( <i>x</i> , <i>y</i> , 0.25) (8 <i>g</i> ) <i>x</i>	0.325(2)	0.313(2)	0.314(2)
Occupancy: 1.00 <i>y</i>	0.273(1)	0.272(1)	0.272(1)
<i>B</i> (Å <sup>2</sup> )	1.5(3)	1.6(3)	1.3(3)
O(3) (0, <i>y</i> , 0.25) (4 <i>c</i> ) <i>y</i>	0.537(4)	0.539(3)	0.540(4)
<i>B</i> (Å <sup>2</sup> )	4.9(9)	3.2(9)	3.5(9)
Occupancy/2	2.02(15)	2.45(12)	2.06(9)

## 2.2. Measurements

The infrared spectra were recorded on a Bruker FTIR spectrophotometer (the samples were dispersed and pressed into KBr pellets) over the frequency range 400–4000 cm<sup>-1</sup>.

The flame emission spectroscopy measurements were carried out at 766.5 nm using a Perkin–Elmer A Analyst 100 spectrophotometer equipped with an air/C<sub>2</sub>H<sub>2</sub> burner. Solid samples were dissolved by adding a minimum of concentrated HCl.

In order to measure the water of crystallization, thermogravimetry (TG) analysis and differential scanning calorimetry (DSC) curves were recorded on a Mettler TC

11 at a heating rate of 5 K min<sup>-1</sup> in air up to 370°C. About 10 mg was weighed into a nickel crucible. Transmission electron microscope (TEM) was used to characterize the morphology of the products.

The X-ray powder diffraction (XRD) analysis was carried out using a Philips diffractometer with CuK<sub>α</sub> radiation. The powder diffraction profiles were collected over the angular range 8° < 2θ < 80° using a 2θ step size of 0.01° at a rate of 0.02° min<sup>-1</sup>. Collected data were analyzed by the Rietveld analysis program (10). Structural investigation was done with Fullprof program (11). No soft constraint on bond distances and angles was imposed. Four coefficients of the Chebyshev polynomial of the first kind describing the background, and the cell parameters, were initially allowed to vary. Atomic coordinates, isotropic thermal parameters were finally freed.

## 3. RESULTS AND DISCUSSION

### 3.1. Structural Determination

3.1.1. *KLnFe(CN)<sub>6</sub>·3.5H<sub>2</sub>O* (*Ln*=Eu, Er, Lu). The XRD data for the three compounds were indexed in

**TABLE 2**  
**Selected Interatomic distances (Å) and Bond Angles for *KLnFe(CN)<sub>6</sub>·3.5H<sub>2</sub>O* (*Ln*=Eu, Er, Lu)**

	<i>Ln</i> =Eu	<i>Ln</i> =Er	<i>Ln</i> =Lu
Fe–C(1) (× 4)	1.91(1)	1.921(8)	1.905(8)
Fe–C(2) (× 2)	1.95(1)	1.89(1)	1.90(1)
Avg.	1.93	1.905	1.903
Ln–O(2)	2.519(6)	2.429(5)	2.427(7)
Ln–O(3)	2.46(2)	2.46(2)	2.48(3)
Avg.	2.49	2.445	2.456
Ln–N(1) (× 4)	2.364(9)	2.301(7)	2.31(1)
Ln–N(2) (× 2)	2.37(1)	2.37(1)	2.36(1)
Avg.	2.368	2.337	2.326
C(1)–N(1)	1.13(1)	1.14(1)	1.15(1)
C(2)–N(2)	1.15(2)	1.18(1)	1.16(2)
Avg.	1.14	1.16	1.155
O(1)–O(2)	2.99(5)	2.92(5)	2.91(4)
O(1)–O(3)	2.73(6)	2.68(5)	2.65(5)
K–O(2)	2.97(3)	2.98(1)	2.95(2)
K–O(3)	2.79(2)	2.77(1)	2.78(2)
N(1)–Ln–N(1)	77.8(4)	78.9(3)	78.3(5)
N(1)–Ln–N(1)'	91.2(4)	92.3(3)	93.0(5)
N(1)–Ln–N(2)	78.5(4)	78.0(4)	77.8(6)
C(1)–Fe–C(1)	91.7(6)	89.1(6)	90.3(7)
C(1)–Fe–C(1)'	88.3(6)	90.9(6)	89.7(8)
C(1)–Fe–C(2)	88.1(8)	89.2(6)	89.6(9)
Avg.	89.4	89.7	89.9
Fe–C(1)–N(1)	178.4(8)	178.0(7)	176.2(9)
Fe–C(2)–N(2)	178.6(12)	176.1(11)	174.1(6)
Ln–N(1)–C(1)	169.4(9)	165.0(9)	163.1(11)
Ln–N(2)–C(2)	179.7(13)	174.4(12)	173.1(15)

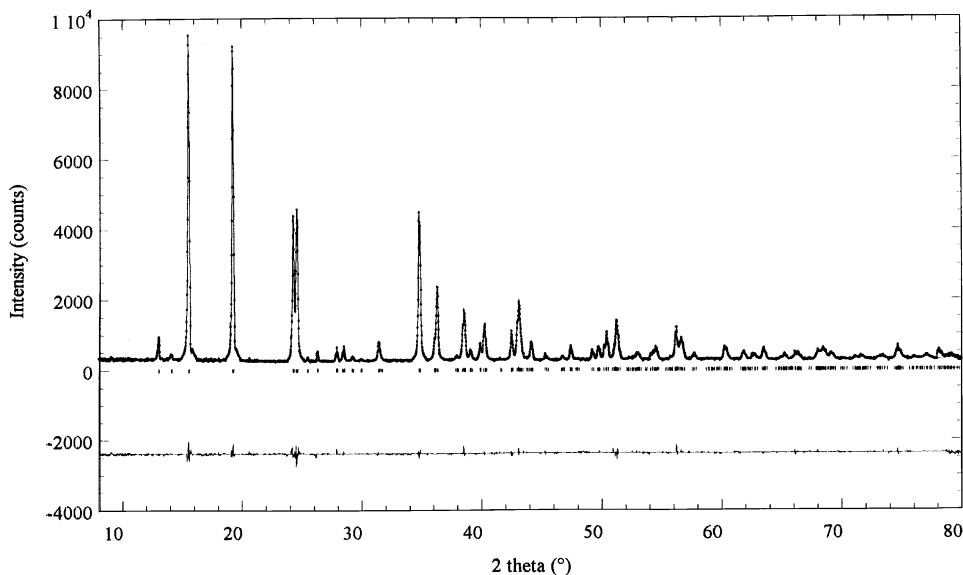


**FIG. 1.** Observed and calculated X-ray diffraction intensity profiles for  $\text{KLnFe(CN)}_6 \cdot 3.5\text{H}_2\text{O}$ . The lower part shows the difference plot,  $I(\text{obs}) - I(\text{calc})$ , and the vertical lines indicate the angular positions of the Bragg reflections.

orthorhombic unit cells; the crystallographic data are shown in Table 1. The similarity in the least-squares refined crystal data shows that they are isostructural with  $\text{KYbFe(CN)}_6 \cdot 3.5\text{H}_2\text{O}$  phase (space group:  $Cmcm$ ) (8). It was observed that the unit-cell parameters decrease from Eu to Lu compound as expected. As a starting point, the Rietveld refinements of powder patterns were carried out using isotropic thermal parameters and atomic positions deduced from the ytterbium compound. The refinements on the basis of the  $Cmcm$  space group were reasonably converged to acceptable values of  $R$  factors. The final atomic coordinates and equivalent isotropic thermal

parameters of each compound are given (Table 1). The result of the pattern fitting for the europium phase is shown in Fig. 1.

The crystal structure of  $\text{KLnFe(CN)}_6 \cdot 3.5\text{H}_2\text{O}$  ( $Ln = \text{Eu, Er, Lu}$ ) is a three-dimensional network of corner-sharing  $\text{FeC}_6$  and  $\text{LnN}_6\text{O}_{2.5}$  units. The six carbons of the pseudo-octahedron  $\text{FeC}_6$  are bound to six surrounding nitrogens of  $\text{LnN}_6\text{O}_{2.5}$  (Fig. 2).

The nine-coordinated lanthanide ion is bound to nitrogen atoms in apical positions (three above and three below the central ion) [range of apical  $Ln-N$  distance: 2.301(7)–2.37(1) Å] and to 2.5 water molecules occupying equatorial capping positions [range of equatorial  $Ln-O$  distance: 2.427(7)–2.519(6) Å] of the distorted trigonal prism (Fig. 3).

The average  $\text{Fe-C}$  (1.90–1.93 Å) and  $\text{C-N}$  (1.14–1.16 Å) bond lengths are nearly the same as reported in the literature data (12). Table 2 lists some bond lengths and angle values. The  $Ln$  groups are linked by non-linear cyanide bridges  $Ln-N-C-Fe$  to  $\text{FeC}_6$  ( $Ln-N-C$ : 163.1–179.7° and  $\text{Fe-C-N}$ : 176.1–178.6°). The non-linear bridging brings a kind of undulation, which generates cavities throughout the structure. These cavities combine into well-defined channels in which the uncoordinated water molecules and potassium ions are located. An important result of the XRD refinement is the confirmation of two crystallographically and chemically distinct kinds of water molecules within the relatively open orthorhombic  $Ln(\text{III})-N-C-Fe(\text{II})$  framework. The first kind of water molecules ( $\text{O}_2$  and  $\text{O}_3$ ) is part of coordination shell of  $Ln(\text{III})$ . The

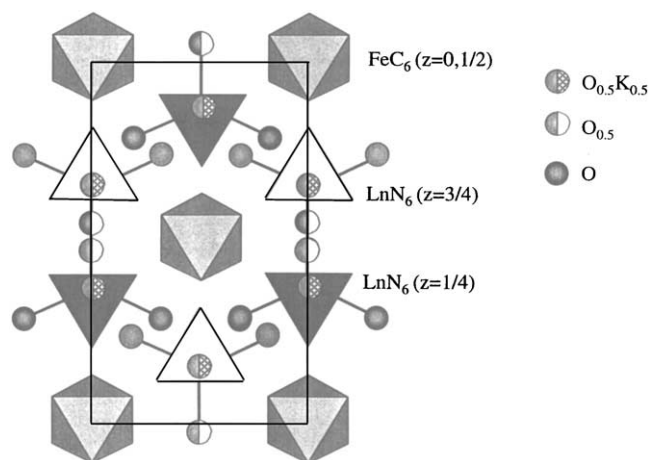


**FIG. 2.** Schematic representation of the  $Ln$  and  $Fe$  polyhedra packing in the cell.

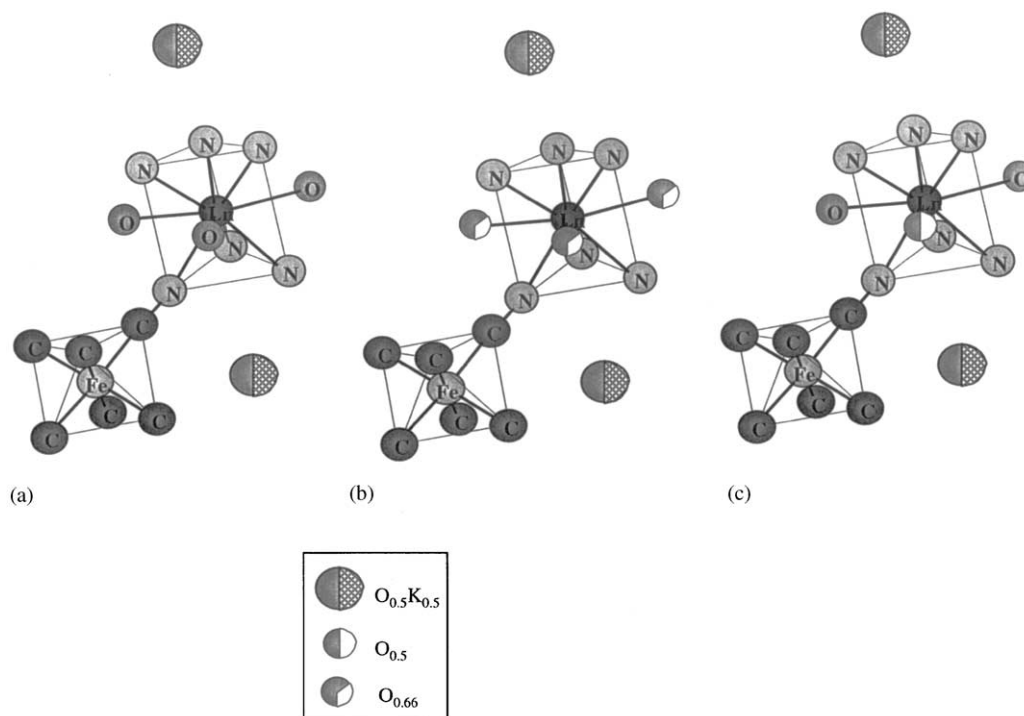


FIG. 3. Local coordination of Fe and Ln atoms in  $KLnFe(CN)_6 \cdot xH_2O$ : (a)  $Ln = La-Nd$ ,  $x = 4$ ; (b)  $Ln = Sm$ ,  $x = 3$ ; and (c)  $Ln = Eu-Lu$ ,  $x = 3.5$ .

second kind (O1) occupies interstitial positions and corresponds therefore to uncoordinated water. For an ideal stoichiometry to be realized in  $KLnFe(CN)_6 \cdot 3.5H_2O$ ,

the unit cell contains 2.5 coordinated and 1 uncoordinated water molecules. The O–O distances are 2.91–2.99 Å for O1–O2 and 2.65–2.73 Å for O1–O3. Only the second

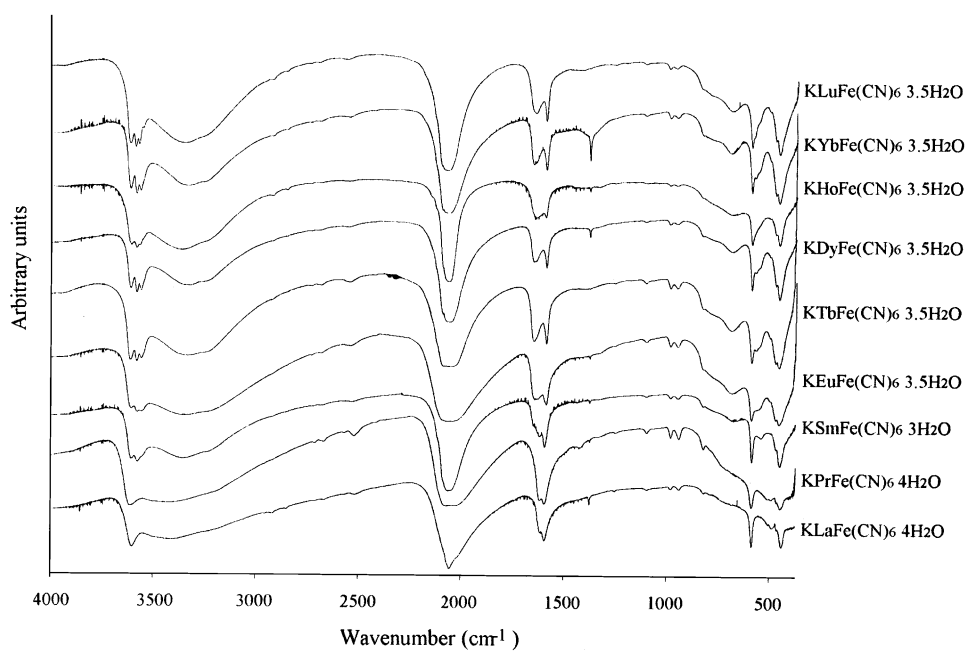


FIG. 4. Infrared absorption spectra of  $KLnFe(CN)_6$ .

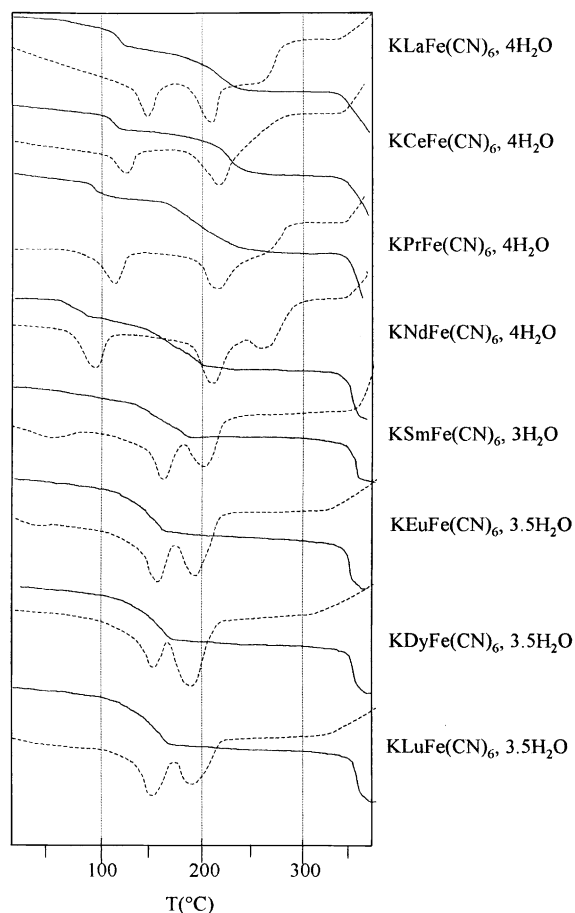


FIG. 5. TGA (solid line) and DSC (broken lines) curves of  $\text{KLnFe(CN)}_6 \cdot x\text{H}_2\text{O}$ .

distance can be considered as a hydrogen bond between the two kinds of water molecules (13).

### 3.2. Spectroscopic Analysis

The comparison of FTIR spectra of the series of lanthanide ferrocyanides leads to the following information (Fig. 4): in all spectra, a strong and broadband absorption due to C–N stretching vibrations is observed (approximately  $2060\text{ cm}^{-1}$ ). The bands at  $405$  and  $600\text{ cm}^{-1}$  are assigned to the stretching mode of Fe–C (of  $\text{FeC}_6$  octahedron) and the bending mode of Fe–C–N, respectively. A strong absorption band between  $3200$  and  $3400\text{ cm}^{-1}$  corresponds to uncoordinated water.

For  $\text{KLnFe(CN)}_6 \cdot 4\text{H}_2\text{O}$  ( $\text{Ln} = \text{La–Nd}$ ) in which three water molecules are coordinated to  $\text{Ln}$  atom, one medium sharp band near  $3600\text{ cm}^{-1}$  characteristic of OH stretching and two medium bands ( $1600\text{–}1620\text{ cm}^{-1}$ ) characteristic of the H–O–H bending appear.

For  $\text{KLnFe(CN)}_6 \cdot x\text{H}_2\text{O}$  ( $\text{Ln} = \text{Sm–Lu}$ ;  $x = 3$  or  $3.5$ ) in which oxygen atoms are partially coordinated to the lanthanide atom, the symmetry is lowered and new types of absorption bands are observed: e.g., splitting of the  $3600\text{ cm}^{-1}$  peak corresponding to the OH stretching frequency for the Sm phase ( $3\text{ H}_2\text{O}$  complex) is accentuated for the  $3.5\text{ H}_2\text{O}$  complexes in agreement with structural results.

### 3.3. Thermal Behavior

Parallel thermogravimetric and differential scanning calorimetry (DSC) analyses of the cyanides were carried

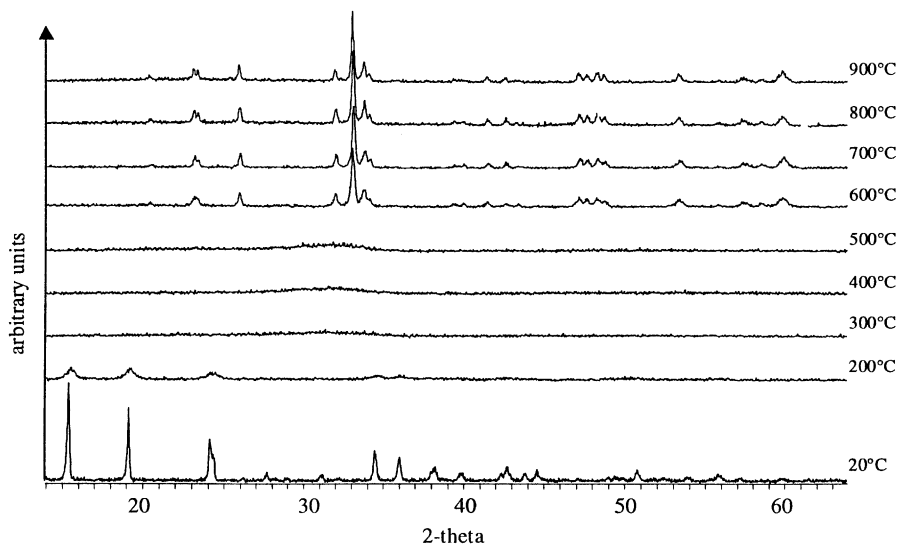


FIG. 6. Powder diffraction patterns for  $\text{KDyFe(CN)}_6 \cdot 3.5\text{H}_2\text{O}$  calcined at different temperatures (the samples were heated at selected temperatures and cooled to room temperature prior to the XRD measurements).

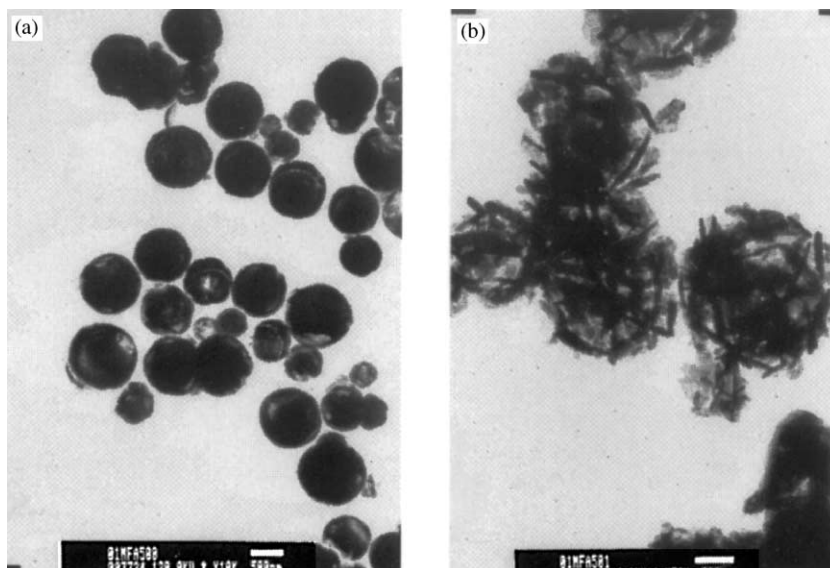


FIG. 7. TEM micrograph top view for (a)  $\text{KDyFe(CN)}_6 \cdot 3.5\text{H}_2\text{O}$  and (b) heat treated at  $800^\circ\text{C}$ .

out. The results show that the lighter lanthanides (La, Ce, Pr and Nd) form tetrahydrates, Sm forms a trihydrate and the other heavier metals (Eu to Lu) lead to 3.5 hydrates.

TG curves of tetrahydrate complexes display two discrete weight loss regions (Fig. 5); they are assigned to the loss of one water molecule at  $120^\circ\text{C}$  followed by the later loss of three water molecules between  $150$  and  $220^\circ\text{C}$ . In lighter lanthanide hydrate TG curves, only one discrete weight loss region is observed which corresponds to the loss of three water molecules for  $\text{Sm}^{3+}$  hydrate and 3.5 molecules for the  $\text{Eu}^{3+}$  to  $\text{Lu}^{3+}$  hydrates respectively.

Endothermic peaks were observed on the DSC curves: (i) the first peak, corresponding to the dehydration of one molecule of coordinated water gradually shifts to lower temperatures from La to Nd tetrahydrate complexes and

disappears for smaller lanthanides. The decrease in the ionic radius of the  $\text{Ln}^{3+}$  series and the subsequent narrowing of the coordination sphere around the  $\text{Ln}^{3+}$  is responsible for an increasing mutual repulsion among ligands which may contribute to the instability of the  $\text{Ln}^{3+}-\text{OH}_2$  bond. (ii) The second and third peaks indicate two types of water molecule bonding (uncoordinated and coordinated).

As the heating process is carried on, an exothermic transformation begins near  $330^\circ\text{C}$  indicating the onset of decomposition and/or the soft decomposition of the precursor.

The XRD patterns of the heat-treated powders were investigated: This process (except for  $\text{Ln}=\text{Ce}$ ) leads to the formation of  $\text{LnFeO}_3$  powders at  $600^\circ\text{C}$  and is illustrated in Fig. 6 for the dysprosium complex together with the XRD

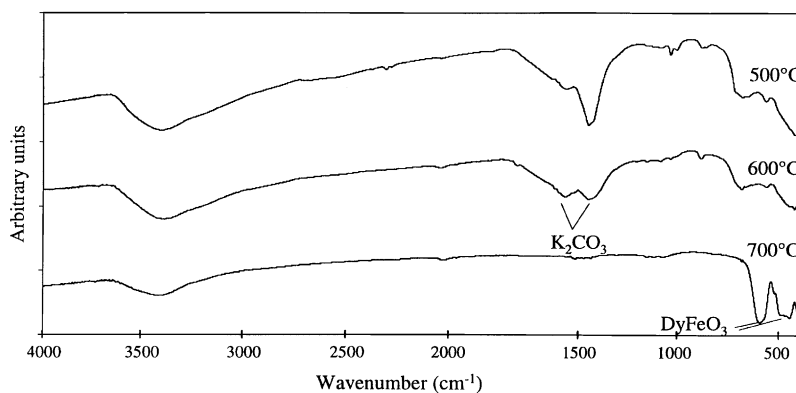


FIG. 8. IR spectra of  $\text{KDyFe(CN)}_6 \cdot 3.5\text{H}_2\text{O}$  heat treated in air at different temperatures.

results and the corresponding decomposition products. Above 600°C, the XRD profiles show only the pattern of the perovskite-type DyFeO<sub>3</sub> (JCPDS file No.37-1493, orthorhombic symmetry, *Pbmm*). The higher the decomposition temperature, the larger the peak intensity and the narrower the peaks. By contrast, a mixture of CeO<sub>2</sub>+Fe<sub>2</sub>O<sub>3</sub> is obtained at 350°C from oxidation of KCeFe(CN)<sub>6</sub>·4H<sub>2</sub>O precursor.

The TEM micrographs obtained for the hexacyanoferrates show that all complexes exhibit particle aggregates with spherical morphology (Fig. 7a); the size distribution being centered around 500 nm. After calcination (Fig. 7b), the morphology of ternary oxides exhibits thin needles 200 nm long and around 20 nm thick.

Gomez *et al.* (14) have clearly demonstrated that the oxidation of CN in hexacyanoferrate is the source of formation of carbonate. This reaction seems to take place at  $T > 350^\circ\text{C}$ ; the presence of carbonate is suggested by IR spectroscopy at 500°C but it disappears at 700°C as shown in Fig. 8. The CO<sub>2</sub> generated *in situ* should therefore be responsible for the K<sub>2</sub>CO<sub>3</sub> production, this latter compound volatilizing above 700°C; this hypothesis is supported by the next to zero potassium content determined by flame emission photometry.

The same temperature dependence studies have been carried out for NaLnFe(CN)<sub>6</sub>·xH<sub>2</sub>O and NH<sub>4</sub>CeFe(CN)<sub>6</sub>·xH<sub>2</sub>O. In both cases, similar results as for KLnFe(CN)<sub>6</sub>·xH<sub>2</sub>O are obtained and ternary oxides are formed near 600°C without Ln<sub>2</sub>O<sub>3</sub> and Fe<sub>2</sub>O<sub>3</sub> products.

Attempts to use lanthanide cyanide complexes for the preparation of ternary nitride were unsuccessful: mixtures of Ln<sub>2</sub>O<sub>3</sub> and FeN (JCPDS No.6 0627) were obtained.

## REFERENCES

1. W. Prandtl and S. Mohr, *Z. Anorg. Allg. Chem.* **236**, 243 (1938).
2. G. W. Beall, D. F. Mullica, W. O. Milligan, J. Korp, and I. Bernal, *Acta Crystallogr. B* **34**, 1446 (1978).
3. D. F. Mullica, W. O. Milligan, and J. D. Oliver, *Inorg. Nucl. Chem. Lett.* **15**, 1 (1979).
4. D. F. Mullica, E. L. Sappenfield, and H. O. Perkins, *J. Solid State Chem.* **73**, 65 (1988).
5. W. O. Milligan, D. F. Mullica, and H. O. Perkins, *Inorg. Chim. Acta* **60**, 35 (1982).
6. W. E. Bailey, R. J. Williams, and W. O. Milligan, *Acta Crystallogr. B* **29**, 1365 (1973).
7. D. F. Mullica, E. L. Sappenfield, and H. O. Perkins, *J. Solid State Chem.* **78**, 301 (1989).
8. D. F. Mullica, E. L. Sappenfield, and T. A. Curnigham, *J. Solid State Chem.* **91**, 98 (1991).
9. S. Nakayama, M. Sakamoto, K. Matsubi, Y. Okimura, R. Ohsumi, Y. Nakayama, and Y. Sadaoka, *Chem. Lett.* 2145 (1992).
10. H. M. Rietveld, *J. Appl. Crystallogr.* **2**, 65 (1969).
11. J. Rodriguez-Carvajal, "FULLPROF: a Program for Rietveld Refinement and Pattern Matching Analysis," Abstracts of the Satellite Meeting on Powder Diffraction of the XV Congress of the IUCr, 127, Toulouse, France, 1990.
12. A. G. Orpen, L. Bramer, F. H. Allen, O. Kennard, D. G. Watson, and R. Taylor, *J. Chem. Soc. Dalton Trans.* **1**, S1 (1989).
13. I. D. Brown, *Acta Crystallogr. A* **32**, 24 (1976).
14. M. I. Gomez, J. A. de Moran, R. E. Carbonio, and P. J. Aymonino, *J. Solid State Chem.* **142**, 138 (1999).